Demonstration of systematic photonic crystal device design and optimization by low-rank adjustments: an extremely compact mode separator

Yang Jiao, Shanhui Fan, and David A. B. Miller

Ginzton Laboratory, Department of Electrical Engineering, Stanford University, Stanford, California 94305-4088

Received August 20, 2004

We present a powerful design and optimization method for devices in a photonic crystal. The method is based on a Wannier basis field expansion and efficient matrix analysis techniques for searching through a vast number of designs. The method permits the design of many compact optical devices with complex and novel functions. We present a design example of a very compact mode separator that is 8.2 μm $\times$ 13.3 μm in size that demultiplexes the three modes of an input photonic crystal multimode waveguide into three single-mode output waveguides. We verify the method with finite-difference time-domain calculations.

OCIS codes: 000.3860, 130.3120, 230.3990, 260.2110.

Currently, the majority of photonic crystal (PC) device designs rely on combining physical insights and innovative modeling with extremely computationally expensive fine tuning. The fine tuning often requires multiple iterations of finite-difference time-domain[1] (FDTD) or plane-wave expansion calculations.[2–4] A number of authors have worked on more-efficient methods for analyzing PC structures.[5,6] In this Letter we introduce a new design method for PC devices. In our method, using modest personal computational hardware, we obtain PC device designs that satisfy arbitrary transmission–reflection characteristics. The method is based on Wannier basis analysis of the device and efficient design optimization by use of a small rank adjustment inverse. We demonstrate our new design paradigm by designing an extremely compact mode demultiplexer. The device separates the three modes of the input waveguide and converts them into the modes of three output single-mode waveguides. As the example will show, the method works even when there is little physical intuition to guide the design.

For clarity, we focus on defect structures in a two-dimensional PC with TM-polarized fields. Extension to the TE case[7] is straightforward. First we expand the field in the Wannier basis as $E(\mathbf{r}) = \sum_{n,\mathbf{R}} a_{n,\mathbf{R}} W_{n,\mathbf{R}}(\mathbf{r})$, where $a_{n,\mathbf{R}}$ are the expansion coefficients and $W_{n,\mathbf{R}}(\mathbf{r})$ are the Wannier functions, with Bloch wave band index n and crystal lattice vector $\mathbf{R}$. Using this expansion in the monochromatic Maxwell equation, after a few matrix manipulations, we get a simple matrix equation for the transmission–reflection of PC defect structures with PC waveguide input–outputs:

$$\mathbf{B}\mathbf{q} = \mathbf{p}\,, \tag{1}$$

where the system matrix $\mathbf{B} \in \mathbb{R}^{k\times k}$ can be calculated from the geometries of the PC defect structure and vector $\mathbf{p}$ is related to the input field; $\mathbf{q}$ is a vector of the form $\{\mathbf{r}, \mathbf{t}, \mathbf{a}\}$, where $\mathbf{r} = r_i$ and $\mathbf{t} = t_i\{i = 1, \ldots, n\}$ are the reflection and transmission coefficients of the input and output waveguide modes, respectively. The number of nonzero expansion coefficients determines the dimension of $\mathbf{B}$. The full form of $\mathbf{B}$ is given by Busch, who proposed this type of formulation for Wannier basis PC structure analysis.[8] What is important for this discussion is that, in the presence of an additional dielectric perturbation $\delta\epsilon(\mathbf{r})$, Eq. (1) changes to

$$(\mathbf{B} + \delta\mathbf{D})\mathbf{q} = \mathbf{p}\,, \tag{2}$$

with

$$(\delta\mathbf{D})_{n\mathbf{R},m\mathbf{S}} = \int_{\mathbb{R}^2} W_{n,\mathbf{R}}{}^{*}(\mathbf{r})\delta\epsilon(\mathbf{r})W_{m,\mathbf{S}}(\mathbf{r})\mathrm{d}^2\mathbf{r}\,. \tag{3}$$

As in any optimization algorithm, we start with an initial guess as to the device design. Matrix $\mathbf{B}$ for the initial device is formed. The transmission–reflection coefficients can then be found with Eq. (1) by finding $\mathbf{B}^{-1}$. Matrix $\mathbf{B}$ is small enough to be inverted directly for structures with as many as 1000 lattice sites. Next we modify design parameters (dielectric distribution of different unit cells) to try to improve the transmission characteristic. After each step, we find the new transmission–reflection coefficients with Eq. (2). We iterate the tuning process until the tolerances on the transmission–reflection coefficients are satisfied.

If we consider only small perturbations to the initial design, then tuning based on the gradient of the transmission with respect to design parameters is appropriate. However, if the initial design is far from the optimum, then a local optimum found by gradient methods is not meaningful. In our algorithm we assume there is little information to guide us in the initial design. In this case a heuristic search algorithm, such as simulated annealing, is more appropriate

0146-9592/05/020141-03$15.00/0

than gradient methods. This simulated annealing also restricts the allowable dielectric distributions of each unit cell to a discrete set. As we will show by an example, if we work with a large number of unit cells, restricting allowable dielectric distributions to a discrete set still allows us to achieve desired transmission–reflection characteristics.

The main cost of the optimization is that one must solve Eq. (2) in each search step. k, the dimension of the system matrix, is typically a few thousand for devices with several hundred lattice sites. In our method we dramatically speed up the search by use of a low-rank matrix inverse update, made possible by the highly localized Wannier basis. We use $\delta\mathbf{D}^{(\alpha,i)}$ $\{\alpha = 1,\ldots,N\}$ to denote the N allowable updates to the dielectric distribution of lattice site i. Because of the localization of the Wannier functions to a few unit cells, $\delta\mathbf{D}^{(\alpha,i)}$ is zero except for lattice sites neighboring lattice site i. Assuming $\delta\mathbf{D}^{(\alpha,i)}$ is nonzero for l neighboring lattice sites, we have

$$\delta\mathbf{D}^{(\alpha,i)} = \mathbf{X}^{(i)}\mathbf{E}^{(\alpha)}\mathbf{Y}^{(i)}, \tag{4}$$

where $\mathbf{X}^{(i)} = [\cdots\mathbf{I}\cdots]^T \in \mathbb{R}^{k\times l}$, $\mathbf{E}^{(\alpha)} \in \mathbb{R}^{l\times l}$, $\mathbf{Y}^{(i)} = [\cdots\mathbf{I}\cdots] \in \mathbb{R}^{l\times k}$, and l is much smaller than k, the full dimension of the system matrix. The rectangular blocks $\mathbf{X}^{(i)}$ and $\mathbf{Y}^{(i)}$ are zero everywhere except for the identity matrices shown. The locations of the identity matrices determine the location of the updated lattice site. We can show using Eq. (3) that $\mathbf{E}^{(\alpha)}$ is independent of the updated lattice site. Matrix $\mathbf{E}^{(\alpha)}$ is typically not well conditioned, i.e., not truly full rank. Therefore we use a singular value decomposition to write

$$\mathbf{E}^{(\alpha)} = \mathbf{V}^{(\alpha)}\mathbf{F}^{(\alpha)}\mathbf{W}^{(\alpha)}, \tag{5}$$

where $\mathbf{V} \in \mathbb{R}^{l\times m}$, $\mathbf{F} \in \mathbb{R}^{m\times m}$, and $\mathbf{W} \in \mathbb{R}^{m\times l}$. From Eq. (5), we see that the rank of the update matrices $\delta\mathbf{D}^{(\alpha,i)}$ are m, which is typically less than 100.

For a possible update, Eq. (1) becomes $[\mathbf{B} + \delta\mathbf{D}^{(\alpha,i)}]\mathbf{q} = \mathbf{p}$. To find the new transmission coefficient we can invert the matrix $[\mathbf{B} + \delta\mathbf{D}^{(\alpha,i)}]$. In our method we dramatically speed up this process by taking advantage of the low rank of $\delta\mathbf{D}^{(\alpha,i)}$. We find $[\mathbf{B} + \delta\mathbf{D}^{(\alpha,i)}]^{-1}$ by use of an expression for the inverse of a small rank adjustment[9]:

$$[\mathbf{B} + \delta\mathbf{D}^{(\alpha,i)}]^{-1} = \mathbf{B}^{-1} - \mathbf{B}^{-1}\mathbf{X}\mathbf{V} \times (\mathbf{F}^{-1}\mathbf{W}\mathbf{Y}\mathbf{B}^{-1}\mathbf{X}\mathbf{V})^{-1}\mathbf{W}\mathbf{Y}\mathbf{B}^{-1}, \tag{6}$$

where $\mathbf{X}$, $\mathbf{Y}$, $\mathbf{V}$, $\mathbf{W}$, and $\mathbf{F}$ are given in Eqs. (4) and (5) and we omit the superscripts for clarity. Despite the longer form, Eq. (6) involves the inversion of two matrices of dimensions $m \times m$ and uses a value of $\mathbf{B}^{-1}$ that was already calculated for the initial design. m is typically less than 100, while the dimension of system matrix $\mathbf{B}$, k, can be several thousand. Because a matrix inversion has a complexity of $O(n^3)$, using Eq. (6) to find the inverse is at least 3 orders of magnitude faster than direct inversion. This speedup means that the simulated-annealing-based heuristic search has become a computationally practical design method for PC devices.

We demonstrate our design method by use of a mode separator design example. We wish to design a device that separates three guiding modes of a multimode waveguide around an operating wavelength of 1503 nm. Previous mode separator designs either used adiabatic mode transformation,[10] which makes the devices very long (>100 μm), or relied on the symmetry of the modes,[11] which limits the separation to odd and even modes. Our design does not have either of these shortcomings. We start with a two-dimensional PC made from high-index cylinders ($n = 3.4$, rod radius $0.18a$, where a is the lattice constant) in air. The initial guess for the design is shown in Fig. 1(a). The input waveguide, made from three rows of missing rods, supports three modes. The three output single-mode waveguides are made from single rows of missing rods. The final design will take the three modes of the input guide and separate them into the three output waveguides. The initial guess is quite arbitrary, however, and the initial structure does not act as a mode separator at all.

Next we search for a better design by removing or adding rods to the design region outlined in Fig. 1(a). At each step the new transmission is calculated with Eq. (6). Each update to the structure involves computing Eq. (6) three times, once for each input mode. The search is done by simulated annealing. In each update the cost function used in the simulated annealing is the sum of the square of all unwanted reflections and transmissions for all three input modes. On a 1-GHz Pentium III computer each update took ~3 s to compute. In comparison, finding the inverse directly takes ~1 h on the same computer.

Figure 1(b) shows the final design with our design method. The final design is found after 48 h of computer time on the same 1-GHz Pentium III computer. Figure 2 shows the field patterns for each input mode at the design frequency. The field patterns are obtained by summing the Wannier functions, with weights found by use of Eq. (2). For all three input

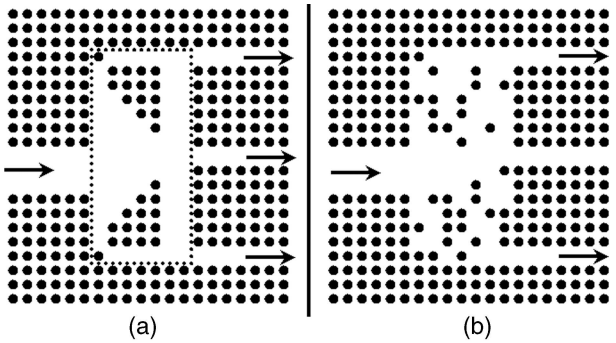

Fig. 1. (a) Initial guess as to the mode separator structure. The PC parameters are given in the text. The arrows show the input and output ports. The dotted rectangle shows the design region of the structure that is altered in the search process. (b) Final design of the mode separator.

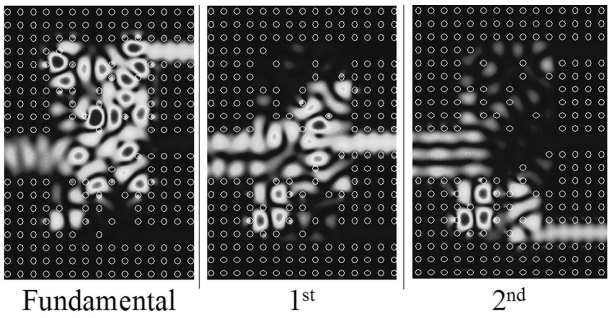

Fig. 2. Mode separator in action. The three field patterns are for each of the three input waveguide modes. Lighter shading indicates a larger field. The structure is superimposed onto the field patterns. The irregularities in the input fields are due to the small reflections (−10 dB) from the device.

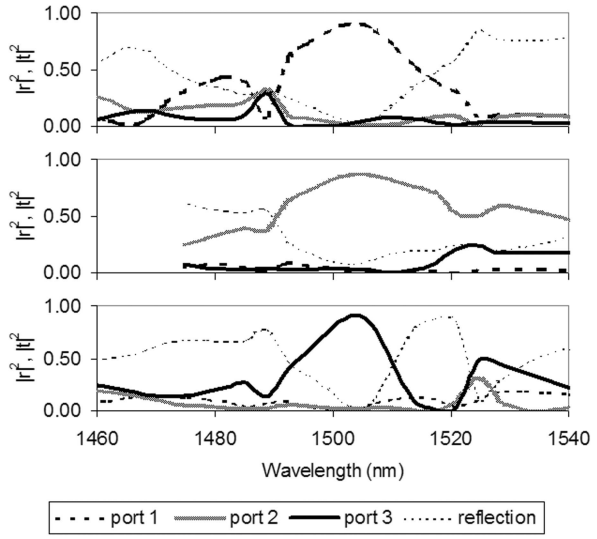

Fig. 3. From top to bottom, the FDTD simulation transmission and reflection spectra for fundamental, first-order, and second-order input waveguide modes. Ports 1–3 refer to the three output waveguides.

modes the contrast ratio of the intended output to the unwanted output is greater than 15 dB. The contrast ratio between the intended output and the reflection is greater than 10 dB. Note that we have restricted our design space to the complete removal or addition of high-index rods to the device region. The rods all have the same index and radius. It may appear that this would severely restrict the achievable characteristics. However, the discretization of the design space is compensated for by the large number of rods in the design region. As shown in Fig. 1(a), 105 rods can be turned on or off in the design process, allowing 2^{105} possible designs. Although arbitrary transmission characteristics are not always achievable, Fig. 1(b) shows that very good transmission characteristics can already be obtained. At this point, if we wish, we can fine tune the design by using a combination of a discrete set of small perturbations and an accelerated gradient method in the Wannier basis, given in our concurrent work.[12]

Figure 3 shows the FDTD calculation of the transmission and reflection for each input mode. The FDTD result confirms that our design functions as a mode separator with low reflection and low cross talk. At the design frequency, the transmission–reflection coefficients found with FDTD calculations agree fairly well with the Wannier basis calculations. Most importantly, the FDTD spectra show that even though we have designed for a single frequency, the resulting device has a working bandwidth of ~5 nm.

The mode demultiplexing device is realized over a region of 13 × 21 lattice constants. For a device operating at 1.5 μm, this means a device size of 8.2 μm × 13.3 μm. In comparison, mode filters using multimode interference couplers are hundreds of micrometers long.[11] It should be noted that the device size that we quote is the area with a nonnegligible field, not just the area with defects. This is the most compact mode separator–converter known to the authors.

In conclusion, we have introduced a highly efficient method for designing PC devices. We have demonstrated the method with a design for a compact mode separator and verified the result with FDTD simulations. Our example is two dimensional. The complexity of our method scales with the number of lattice sites used, independent of the number of computational grid points in each unit cell. Therefore, if maximally localized Wannier functions are constructed for three-dimensional PCs, the method should apply with little additional computational complexity. This method will permit the design of a vast variety of compact photonic devices with novel and complex functions.

Y. Jiao's e-mail address is jiaoyang@stanford.edu.

References

1. A. Taflove and S. C. Hagness, *Computational Electrodynamics: the Finite-Difference Time-Domain Method*, 2nd ed. (Artech House, Norwood, Mass., 2000).
2. S. G. Johnson and J. D. Joannopoulos, Opt. Express **8,** 173 (2001), http://www.opticsexpress.org.
3. R. Wilson, T. J. Karle, I. Moerman, and T. F. Krauss, J. Opt. A Pure Appl. Opt. **5,** S76 (2003).
4. J. Vuckovic, M. Loncar, H. Mabuchi, and A. Scherer, IEEE J. Quantum Electron. **38,** 850 (2002).
5. Z. Y. Li and K. M. Ho, Phys. Rev. B **68,** 155101 (2003).
6. E. Moreno, D. Erni, and C. Hafner, Phys. Rev. E **66,** 036618 (2002).
7. J. P. Albert, C. Jouanin, D. Cassagne, and D. Bertho, Phys. Rev. B **61,** 4381 (2000).
8. K. Busch, S. F. Mingaleev, A. Garcia-Martin, M. Schillinger, and D. Hermann, J. Phys. Condens. Matter **15,** R1233 (2003).
9. R. A. Horn and C. R. Johnson, *Matrix Analysis* (Cambridge U. Press, Cambridge, England, 1990), p. 561.
10. B. T. Lee and S. Y. Shin, Opt. Lett. **28,** 1660 (2003).
11. J. Leuthold, J. Eckner, E. Gamper, P. A. Besse, and H. Melchior, J. Lightwave Technol. **16,** 1228 (1998).
12. Y. Jiao, S. Fan, and D. A. B. Miller, "Photonic crystal device sensitivity analysis with Wannier basis gradients," Opt. Lett. (to be published).